Robust Fault Diagnosis for Systems with Electronic Induced Delays

Robert Fonod, David Henry, Eric Bornschlegl, Catherine Charbonnel

Robust Fault Diagnosis for Systems with Electronic Induced Delays

R. Fonod [*] **D. Henry** [*] **E. Bornschlegl** [**] **C. Charbonnel** [***]

[*] *University Bordeaux 1 - IMS-LAPS, Bordeaux, France*
{robert.fonod,david.henry}@ims-bordeaux.fr
[**] *European Space Agency, Noordwijk, The Netherlands*
eric.bornschlegl@esa.int
[***] *Thales Alenia Space, Cannes, France*
catherine.charbonnel@thalesaleniaspace.com

Abstract:
A problem of robust fault diagnosis of digital controlled continuous-time systems with uncertain time-varying input delay is studied in this paper. Two residual-based fault detection and isolation (FDI) schemes are proposed that are robust in terms of time-varying delays induced by the electronic devices and disturbances. The idea of both proposed methods is to transform the uncertainty caused by delays into unknown inputs and decouple them by means of eigenstructure assignment (EA) technique. The first method utilizes a Cayley-Hamilton theorem based transformation and the second relies on a first-order Padé approximation of the time delay. Finally, the applicability and effectiveness of the proposed methods is illustrated through simulation results from the "high-fidelity" industrial simulator, provided by Thales Alenia Space.

Keywords: Fault diagnosis; Uncertainty; Eigenstructure assignment; Electronic induced delay.

ACRONYMS

EA Eigenstructure Assignment
FDI Fault Detection and Isolation
IMU Inertial Measurement Unit
LIDAR LIght Detection And Ranging
MAV Mars Ascent Vehicle
MSR Mars Sample Return
RW Reaction Wheels
STR Star TRacker
SVD Singular Value Decomposition
THR THRuster
UI Unknown Input

1. INTRODUCTION

In recent years, due to the increased complexity, as well as the need for reliability, safety, and efficient operation of industrial and aerospace systems, a great deal of attention has been paid to the subject of fault detection and isolation (FDI) in dynamic systems. A great number of methods for FDI have been proposed (see Chen and Patton [1999], Blanke et al. [2006], Ding [2008] and the references therein). Only a limited results on FDI of time-delay systems have been developed in recent years.In Yang and Saif [1998], an unknown input observer is designed for fault detection of state-delayed systems with known delays. Robust fault detector design problem is investigated in Karimi et al. [2010] for a class of linear systems with some nonlinear perturbations and mixed neutral and discrete time-varying delays. Recently, a geometric approach for FDI of retarded and neutral time-delay systems was developed in Meskin and Khorasani [2009].

One of the main difficulties in fault detection of systems subject to uncertain time-varying delay lies in the fact that influence caused by electronic-induced input delay is unstructured, therefore robustness to influence caused by such delays cannot be ensured by applying existing robust FDI approaches directly. In this paper, by introducing a Cayley-Hamilton theorem based (see e.g. Wang et al. [2008]) and Padé approximation based transformation, influence of uncertain time-varying delay is transformed into unknown inputs, which as shown, greatly facilitates the above mentioned difficulty.

Two residual generator based FDI schemes are proposed for a class of linear systems with disturbances. The system is modelled as a continuous-time one with digital control, where the control input has a piecewise-continuous delay. Modelling of continuous-time systems with digital control and delayed control input was introduced by Mikheev et al. [1988]. At the end, the disturbance vector and the unknown input, that models the uncertainty caused by time-varying delays, are lumped together and decoupled by means of Eigenstructure Assignment (EA) technique.

The applicative support of this paper concerns the Mars Sample Return (MSR) mission. Simulation results from the MSR "high-fidelity" industrial simulator demonstrates the efficiency and capabilities of the proposed schemes.

Notations: Let $\mathbb{R}$, $\mathbb{R}^+$ and $\mathbb{Z}^+$ denote the field of real numbers, the set of non-negative reals and the set of non-negative integers, respectively. The notation $\mathbb{R}^{m\times n}$ is used for real matrices of dimension $m \times n$. The Euclidean norm is used for vectors and is written without subscript; e.g. $\|x\|$. By $\boldsymbol{I}$ (or $\mathbf{0}$) we denote the identity (the null) matrix.

2. PROBLEM FORMULATION

Consider a continuous-time system given by

$$\begin{aligned}\dot{\boldsymbol{x}}(t) &= \boldsymbol{A}\boldsymbol{x}(t) + \boldsymbol{B}\boldsymbol{u}(t) + \boldsymbol{E}_f\boldsymbol{f}(t) + \boldsymbol{E}_{d_1}\boldsymbol{d}^1(t)\\ \boldsymbol{y}(t) &= \boldsymbol{C}\boldsymbol{x}(t)\end{aligned} \tag{1}$$

where $\boldsymbol{x}(t) \in \mathbb{R}^n$ is the state vector, $\boldsymbol{u}(t) \in \mathbb{R}^{n_u}$ is the system input vector, $\boldsymbol{y}(t) \in \mathbb{R}^{n_y}$ is the output vector, $\boldsymbol{d}^1(t) \in \mathbb{R}^{n_d}$ and $\boldsymbol{f}(t) \in \mathbb{R}^{n_f}$ are the unknown disturbance and the fault vector. $\boldsymbol{A}$, $\boldsymbol{B}$, $\boldsymbol{C}$, $\boldsymbol{E}_f$ and $\boldsymbol{E}_{d_1}$ are known matrices of appropriate dimensions. The pair $(\boldsymbol{A}, \boldsymbol{C})$ is assumed to be observable.

Suppose that the closed-loop system is controlled by discrete-time controller, and the sampling time is $T \in \mathbb{R}^+$. Since there is an electronic-induced delay $\tau_k \in \mathbb{R}^+, \forall k \in \mathbb{Z}^+$, the controller signal $\boldsymbol{u}_k^c \in \mathbb{R}^{n_u}, k \in \mathbb{Z}^+$ generated at $t = t_k = kT, k \in \mathbb{Z}^+$ arrives at the actuator at time instant $t_k + \tau_k$. Recalling the fact, every control signal $\boldsymbol{u}_k^c$ is held by a zero-order holder and only valid over the interval $[t_k + \tau_k, t_{k+1} + \tau_{k+1})$, we have

$$\boldsymbol{u}(t) = \begin{cases} \boldsymbol{u}_k^c, \ \forall t \in [t_k + \tau_k, t_{k+1} + \tau_{k+1}) \\ \boldsymbol{u}_0^c, \ \forall t \in [0, \tau_1) \end{cases} \tag{2}$$

Problem 1. Design a residual generator that is robust in the presence of uncertain time-varying delay τ_k and unknown input $\boldsymbol{d}^1(t)$.

In order to solve Problem 1, two approaches are presented in this paper. The aim of both approaches is to model the influence of the uncertain time-varying delay as an unknown input (UI). The first approach uses a Cayley-Hamilton theorem based transformation and the second one utilizes a first-order Padé approximation. Then, the unknown inputs are decoupled by means of Eigenstructure Assignment (EA) technique.

3. TRANSFORMATION INTO POLYTOPIC UNCERTAINTY

In this section, we assume that the electronic-induced delay is represented by $\tau_k = lT + \delta_k \leq \bar{\tau}, \forall k \in \mathbb{Z}^+$, where $l \in \mathbb{Z}^+$ is a known constant integer, $\bar{\tau} \in \mathbb{R}^+$ is the upper bound of τ_k and $\delta_k \in \mathbb{R}^+, \forall k \in \mathbb{Z}^+$ is the unknown time varying part of the delay, bounded by $0 \leq \delta_k < mT$ with $m \in \mathbb{Z}^+$ being a known integer. In the next, we assume that $m = 1$.

Remark 1. The case when the variation part of the delay is larger than one sampling period, i.e. $m > 1$, is discussed in Wang et al. [2008].

Consider the discrete representation of (1) over a sampling period

$$\begin{aligned}\boldsymbol{x}_{k+1} &= \bar{\boldsymbol{A}}\boldsymbol{x}_k + \boldsymbol{\Gamma}_0^{\delta_k}\boldsymbol{u}_{k-l}^c + \boldsymbol{\Gamma}_1^{\delta_k}\boldsymbol{u}_{k-l-1}^c + \bar{\boldsymbol{E}}_f\boldsymbol{f}_k + \bar{\boldsymbol{E}}_{d_1}\boldsymbol{d}_k^1\\ \boldsymbol{y}_k &= \bar{\boldsymbol{C}}\boldsymbol{x}_k\end{aligned} \tag{3}$$

where

$$\bar{\boldsymbol{A}} = e^{\boldsymbol{A}T}, \ \boldsymbol{\Gamma}_0^{\delta_k} = \int_0^{T-\delta_k} e^{\boldsymbol{A}t}dt\boldsymbol{B}, \ \bar{\boldsymbol{E}}_{d_1} = \int_0^T e^{\boldsymbol{A}t}dt\boldsymbol{E}_{d_1}$$

$$\bar{\boldsymbol{C}} = \boldsymbol{C}, \quad \boldsymbol{\Gamma}_1^{\delta_k} = \int_{T-\delta_k}^T e^{\boldsymbol{A}t}dt\boldsymbol{B}, \ \bar{\boldsymbol{E}}_f = \int_0^T e^{\boldsymbol{A}t}dt\boldsymbol{E}_f$$

Let $\bar{\boldsymbol{B}} = \int_0^T e^{\boldsymbol{A}t}dt\boldsymbol{B}$, then it follows:

$$\boldsymbol{\Gamma}_0^{\delta_k} + \boldsymbol{\Gamma}_1^{\delta_k} = \int_0^T e^{\boldsymbol{A}t}dt\boldsymbol{B} = \bar{\boldsymbol{B}} \tag{4}$$

Furthermore, using (3) and (4), and introducing a new augmented state vector of the form $\boldsymbol{z}_k^T = \left[\ \boldsymbol{x}_k^T \ \ (\boldsymbol{u}_{k-l-1}^c)^T\ \right]$ we obtain:

$$\begin{aligned}\boldsymbol{z}_{k+1} &= \hat{\boldsymbol{A}}^{\tau_k}\boldsymbol{z}_k + \hat{\boldsymbol{B}}^{\tau_k}\boldsymbol{u}_{k-l}^c + \hat{\boldsymbol{E}}_f\boldsymbol{f}_k + \hat{\boldsymbol{E}}_{d_1}\boldsymbol{d}_k^1\\ \boldsymbol{y}_k &= \hat{\boldsymbol{C}}\boldsymbol{z}_k\end{aligned} \tag{5}$$

where

$$\hat{\boldsymbol{A}}^{\delta_k} = \begin{bmatrix} \bar{\boldsymbol{A}} & \boldsymbol{\Gamma}_1^{\delta_k} \\ \boldsymbol{0} & \boldsymbol{0} \end{bmatrix}, \ \hat{\boldsymbol{B}}^{\delta_k} = \begin{bmatrix} \bar{\boldsymbol{B}} - \boldsymbol{\Gamma}_1^{\delta_k} \\ \boldsymbol{I} \end{bmatrix}, \ \hat{\boldsymbol{C}} = \begin{bmatrix} \bar{\boldsymbol{C}} & \boldsymbol{0} \\ \boldsymbol{0} & \boldsymbol{I} \end{bmatrix}$$

$$\hat{\boldsymbol{E}}_{d_1} = \begin{bmatrix} \bar{\boldsymbol{E}}_{d_1} \\ \boldsymbol{0} \end{bmatrix}, \quad \hat{\boldsymbol{E}}_f = \begin{bmatrix} \bar{\boldsymbol{E}}_f \\ \boldsymbol{0} \end{bmatrix}$$

In this model $\boldsymbol{\Gamma}_1^{\delta_k}$ is strongly dependent on the uncertain time-varying delay part δ_k. Therefore, the previous system is an uncertain systems with time-varying uncertainty. The challenge that remains is to find a transformation of this uncertainty in order to reformulate (5) into a time-dependent polytopic uncertainty.

3.1 Expressing uncertainties as polytopes of matrices

In this paper, a Cayley-Hamilton theorem based transformation is introduced (see Wang et al. [2008]).

Theorem 1. Let $\boldsymbol{A}$ be a constant matrix with the characteristic polynomial

$$p(\lambda) = \det(\lambda\boldsymbol{I} - \boldsymbol{A}) = \lambda^n + c_{n-1}\lambda^{n-1} + \ldots + c_1\lambda + c_0 \tag{6}$$

then $e^{\boldsymbol{A}t}$ can be written as

$$e^{\boldsymbol{A}t} = s_1(t)\boldsymbol{I} + s_2(t)\boldsymbol{A} + \ldots + s_n(t)\boldsymbol{A}^{n-1} \tag{7}$$

where $s_i(t)$, $1 \leq i \leq n$ are solutions to the n^{th} order homogenous scalar differential equation

$$s^{(n)}(t) + c_{n-1}s^{(n-1)}(t) + \ldots + c_1s'(t) + c_0s(t) = 0 \tag{8}$$

satisfying the following initial conditions:

$$\left.\begin{matrix} s_1(0) = 1 \\ s_1'(0) = 0 \\ \vdots \\ s_1^{n-1}(0) = 0 \end{matrix}\right\}, \left.\begin{matrix} s_2(0) = 0 \\ s_2'(0) = 1 \\ \vdots \\ s_2^{n-1}(0) = 0 \end{matrix}\right\}, \ldots, \left.\begin{matrix} s_n(0) = 0 \\ s_n'(0) = 0 \\ \vdots \\ s_n^{n-1}(0) = 1 \end{matrix}\right\}$$

Proof. The proof can be found in Leonard [1996]. □

Proposition 1. The Cayley-Hamilton theorem based transformation of $\boldsymbol{\Gamma}_1^{\delta_k}$ can be expressed as the convex matrix polytopes

$$\begin{aligned}\boldsymbol{\Gamma}_1^{\delta_k} &= \sum_{i=1}^{2n} \mu_i^k\boldsymbol{U}_i, \qquad \sum_{i=1}^{2n} \mu_i^k = 1\\ \mu_i^k &> 0, \qquad \forall i = 1, \ldots, 2n, \forall k \in \mathbb{Z}^+\end{aligned} \tag{9}$$

where $\boldsymbol{U}_i$ and μ_i^k will be defined later.

Proof. Using (7), we have

$$\boldsymbol{\Gamma}_1^{\delta_k} = \int_{T-\delta_k}^T e^{\boldsymbol{A}t}dt\boldsymbol{B} = \sum_{i=1}^n \left[\left(\int_{T-\delta_k}^T s_i(t)dt \right) \boldsymbol{A}^{i-1}\boldsymbol{B} \right] \tag{10}$$

Define

$$s_i^{\max} = \max_{0\le\delta_k\le T} \int_{T-\delta_k}^{T} s_i(t)dt, \quad i = 1, 2, \ldots, n$$

and

$$s_i^{\min} = \min_{0\le\delta_k\le T} \int_{T-\delta_k}^{T} s_i(t)dt, \quad i = 1, 2, \ldots, n$$

then (10) can be rewritten as

$$\boldsymbol{\Gamma}_1^{\delta_k} = \sum_{i=1}^{n} \left(\alpha_{i,0}^k s_i^{\min} + \alpha_{i,1}^k s_i^{\max}\right) \boldsymbol{A}^{i-1}\boldsymbol{B} \tag{11}$$

where $\alpha_{i,0}^k$ and $\alpha_{i,1}^k$ are two time-varying unknown parameters satisfying $0\le\alpha_{i,0}^k\le 1$, $0\le\alpha_{i,1}^k\le 1$, and $\alpha_{i,0}^k+\alpha_{i,1}^k = 1$.

It can be verified that $\int_{T-\delta_k}^{T} s_i(t)dt, i = 1, 2, \ldots, n$ are Lipschitz-continuous on $0 \le \delta_k \le T$, that is, they satisfy the relation

$$\left| \int_{T-\delta_k^1}^{T} s_i(t)dt - \int_{T-\delta_k^2}^{T} s_i(t)dt \right| \le L_i \left|\delta_k^1 - \delta_k^2\right|$$

for all δ_k^1 and δ_k^2 in $[0, T]$, where $|\cdot|$ denotes the absolute value and $L_i, i = 1, 2, \ldots, n$ are the Lipschitz constants.

Remark 2. Note that the Lipschitz constants are not unique, they can be any finite constants satisfying the above inequality. Therefore, when s_i^{max} and s_i^{min} can not be obtained analytically, reliable Lipschitz global optimization algorithms (e.g., Piyavskii's algorithm), which can guarantee a global convergence for all Lipschitz-continuous functions in a closed interval Pintér [1996], can be adopted to find $s_i^{\max}$ and $s_i^{\min}$ no matter $s_i(t)$, $i = 1, 2, \ldots, n$ are convex or not.

Setting

$$\begin{array}{ll} \mu_{2i-1}^k = \alpha_{i,0}^k/n, & \boldsymbol{U}_{2i-1} = n s_i^{\min}\boldsymbol{A}^{i-1}\boldsymbol{B} \\ \mu_{2i}^k = \alpha_{i,1}^k/n, & \boldsymbol{U}_{2i} = n s_i^{\max}\boldsymbol{A}^{i-1}\boldsymbol{B} \end{array} \tag{12}$$

From (10) and (11), with the notation (12) Proposition 1 is proved. □

Therefore, considering Proposition 1, the system (5) can be rewritten as a polytopic uncertain system

$$\begin{aligned} \boldsymbol{z}_{k+1} &= \left(\hat{\boldsymbol{A}}_0 + \sum_{i=1}^{2n} \mu_i^k \hat{\boldsymbol{A}}_i\right) \boldsymbol{z}_k + \\ &+ \left(\hat{\boldsymbol{B}}_0 + \sum_{i=1}^{2n} \mu_i^k \hat{\boldsymbol{B}}_i\right) \boldsymbol{u}_{k-l}^c + \hat{\boldsymbol{E}}_f \boldsymbol{f}_k + \hat{\boldsymbol{E}}_{d_1} \boldsymbol{d}_k^1 \\ \boldsymbol{y}_k &= \hat{\boldsymbol{C}}\boldsymbol{z}_k \end{aligned} \tag{13}$$

where

$$\hat{\boldsymbol{A}}_0 = \begin{bmatrix} \bar{\boldsymbol{A}} & \boldsymbol{0} \\ \boldsymbol{0} & \boldsymbol{0} \end{bmatrix}, \quad \hat{\boldsymbol{A}}_i = \begin{bmatrix} \boldsymbol{0} & \boldsymbol{U}_i \\ \boldsymbol{0} & \boldsymbol{0} \end{bmatrix}$$
$$\hat{\boldsymbol{B}}_0 = \begin{bmatrix} \bar{\boldsymbol{B}} \\ \boldsymbol{I} \end{bmatrix}, \quad \hat{\boldsymbol{B}}_i = \begin{bmatrix} -\boldsymbol{U}_i \\ \boldsymbol{0} \end{bmatrix}$$

and the rest parameters are the same with those in (5).

Remark 3. Other transformation can be found in the literature, for instance, in Hetel et al. [2006] makes use of a Taylor series expansion of the uncertainty $\boldsymbol{\Gamma}_1^{\delta_k}$, i.e.:

$$\boldsymbol{\Gamma}_1^{\delta_k} = \left(-\sum_{i=1}^{\infty} \frac{(-\delta_k)^i}{i!} \boldsymbol{A}^{i-1} e^{\boldsymbol{A}T}\right) \boldsymbol{B}$$

Other methods, as the ones in Olaru and Niculescu [2008], are based on the Jordan normal form, i.e. $\boldsymbol{A} = \boldsymbol{V}\boldsymbol{J}\boldsymbol{V}^{-1}$, when $\boldsymbol{\Gamma}_1^{\delta_k}$ is expressed as:

$$\boldsymbol{\Gamma}_1^{\delta_k} = \sum_{i=1}^{n} \boldsymbol{A}^{-1}\boldsymbol{V}(e^{\boldsymbol{J}_i T} - e^{\boldsymbol{J}_i(T-\delta_k)})\boldsymbol{V}^{-1}\boldsymbol{B}$$

Remark 4. From the derivation above, it can be concluded that the number of vertices of the polytopic representation is $2n$, which is a linear function of the system order.

3.2 Expressing polytopic uncertainty as an unknown input

The time-varying parts of (13), where $\hat{\boldsymbol{A}}_i$ and $\hat{\boldsymbol{B}}_i$ are known constant matrices, μ_i^k is an unknown scalar time-varying factor, in this case, can be approximated by the disturbance term as in Chen and Patton [1999] by:

$$\begin{aligned} \hat{\boldsymbol{E}}_{d_2}\boldsymbol{d}_k^2 &= \sum_{i=1}^{2n} \mu_i^k \hat{\boldsymbol{A}}_i \boldsymbol{z}_k + \sum_{i=1}^{2n} \mu_i^k \hat{\boldsymbol{B}}_i \boldsymbol{u}_{k-l}^c = \\ &= \underbrace{\left[\hat{\boldsymbol{A}}_1, \ldots, \hat{\boldsymbol{A}}_{2n}, \hat{\boldsymbol{B}}_1, \ldots, \hat{\boldsymbol{B}}_{2n}\right]}_{\hat{\boldsymbol{E}}_{d_2}} \underbrace{\begin{bmatrix} \mu_1^k \boldsymbol{z}_k \\ \vdots \\ \mu_{2n}^k \boldsymbol{z}_k \\ \mu_1^k \boldsymbol{u}_{k-l}^c \\ \vdots \\ \mu_{2n}^k \boldsymbol{u}_{k-l}^c \end{bmatrix}}_{\boldsymbol{d}_k^2} \end{aligned}$$

Now, the two unknown inputs $\boldsymbol{d}_k^1$ and $\boldsymbol{d}_k^2$ can be lumped together, and defined to be $\boldsymbol{d}_k$. That is

$$\boldsymbol{d}_k = \left[\, (\boldsymbol{d}_k^1)^T \;\; (\boldsymbol{d}_k^2)^T \,\right]^T \tag{14}$$

Correspondingly, the UI distribution matrix is

$$\hat{\boldsymbol{E}}_d = \left[\, \hat{\boldsymbol{E}}_{d_1} \;\; \hat{\boldsymbol{E}}_{d_2} \,\right] \tag{15}$$

Taking the above notation into account, the design model is expressed in terms of lumped unknown inputs as

$$\begin{aligned} \boldsymbol{z}_{k+1} &= \hat{\boldsymbol{A}}_0 \boldsymbol{z}_k + \hat{\boldsymbol{B}}_0 \boldsymbol{u}_{k-l}^c + \hat{\boldsymbol{E}}_f \boldsymbol{f}_k + \hat{\boldsymbol{E}}_d \boldsymbol{d}_k \\ \boldsymbol{y}_k &= \hat{\boldsymbol{C}}\boldsymbol{z}_k \end{aligned} \tag{16}$$

This model represents the discrete-time model of the original system (1), that takes into account both disturbances $\boldsymbol{d}_k^1$ and uncertainties caused by electronic-induced delays represented as an additional unknown input $\boldsymbol{d}_k^2$.

4. PADÉ APPROXIMATION

In this section, we assume that the piecewise-constant delay τ_k is represented by time-varying piecewise continuous (continuous from the right) delay $\tau(t) = \tau_k, \forall t \in [t_k, t_{k+1})$. In this sense, the system input (2) is expressed as

$$\boldsymbol{u}(t) = \boldsymbol{u}^c(t - \tau(t)) \tag{17}$$

where $\boldsymbol{u}^c(t) = \boldsymbol{u}_k^c, \forall t \in [t_k, t_{k+1})$ is the control signal.

The transfer function of the time delay is

$$H(s) = e^{-\tau(t)s} \tag{18}$$

This transfer function is irrational and it is necessary to substitute $e^{-\tau(t)s}$ with an approximation in form of a rational transfer function. The most common approximation is the Padé approximation

$$e^{-\tau(t)s} \doteq \frac{1 - k_1 s + k_2 s^2 + \ldots \pm k_n s^n}{1 + k_1 s + k_2 s^2 + \ldots + k_n s^n} \tag{19}$$

where n is the order of the approximation and the coefficients k_i are functions of n.

In this paper, a first-order Padé approximation of the time-varying delay $\tau(t)$ is used, when $k_1 = \frac{\tau(t)}{2}$ and $k_i = 0, i = 2, \ldots, n$, that is:

$$e^{-\tau(t)s} \doteq \frac{1 - \frac{\tau(t)}{2}s}{1 + \frac{\tau(t)}{2}s} \tag{20}$$

If we consider all system inputs, the transfer function (20) is equivalent with the following state space representation

$$\begin{aligned} \dot{\boldsymbol{x}}_d(t) &= \boldsymbol{A}_d(t)\boldsymbol{x}_d(t) + \boldsymbol{B}_d\boldsymbol{u}^c(t) \\ \boldsymbol{u}(t) &= \boldsymbol{C}_d(t)\boldsymbol{x}_d(t) + \boldsymbol{D}_d\boldsymbol{u}^c(t) \end{aligned} \tag{21}$$

where $\boldsymbol{x}_d(t) \in \mathbb{R}^{n_u}$ is the delayed state and $\boldsymbol{A}_d(t) = -\frac{2}{\tau(t)}\boldsymbol{I}, \boldsymbol{B}_d = \boldsymbol{I}, \boldsymbol{C}_d(t) = \frac{4}{\tau(t)}\boldsymbol{I}, \boldsymbol{D}_d = -\boldsymbol{I}$ are matrices with appropriate dimension.

The augmented state-space description of the system (1) and the delayed inputs (21) is:

$$\begin{aligned} \dot{\boldsymbol{z}}(t) &= \hat{\boldsymbol{A}}(t)\boldsymbol{z}(t) + \hat{\boldsymbol{B}}\boldsymbol{u}(t) + \hat{\boldsymbol{E}}_f\boldsymbol{f}(t) + \hat{\boldsymbol{E}}_{d_1}\boldsymbol{d}^1(t) \\ \boldsymbol{y}(t) &= \hat{\boldsymbol{C}}\boldsymbol{z}(t) \end{aligned} \tag{22}$$

where

$$\hat{\boldsymbol{A}}(t) = \begin{bmatrix} \boldsymbol{A} & \boldsymbol{B}\boldsymbol{C}_d(t) \\ \boldsymbol{0} & \boldsymbol{A}_d(t) \end{bmatrix}, \quad \hat{\boldsymbol{B}} = \begin{bmatrix} \boldsymbol{B}\boldsymbol{D}_d \\ \boldsymbol{B}_d \end{bmatrix}, \quad \hat{\boldsymbol{C}} = [\,\boldsymbol{C}\ \boldsymbol{0}\,]$$

$$\boldsymbol{z}(t) = \begin{bmatrix} \boldsymbol{x}(t) \\ \boldsymbol{x}_d(t) \end{bmatrix}, \qquad \hat{\boldsymbol{E}}_f = \begin{bmatrix} \boldsymbol{E}_f \\ \boldsymbol{0} \end{bmatrix}, \quad \hat{\boldsymbol{E}}_{d_1} = \begin{bmatrix} \boldsymbol{E}_{d_1} \\ \boldsymbol{0} \end{bmatrix}$$

It can be seen, that the uncertainty is present only in $\hat{\boldsymbol{A}}(t)$, thus the task is to decompose this matrix into the constant and time-varying part and to model the uncertainty part as an UI.

4.1 Expressing uncertainty as an unknown input

Problem 2. Decompose the matrix $\hat{\boldsymbol{A}}(t)$ into two parts:

$$\hat{\boldsymbol{A}}(t) = \hat{\boldsymbol{A}}_0 + \Delta\hat{\boldsymbol{A}}(t) \tag{23}$$

where $\hat{\boldsymbol{A}}_0$ is a constant matrix and $\Delta\hat{\boldsymbol{A}}(t)$ is the time-varying part of $\hat{\boldsymbol{A}}(t)$.

Consider, that $\tau(t)$ can be expressed as

$$\tau(t) = \tau_0 + \Delta\tau(t) \ : \ |\Delta\tau(t)| \leq \bar{\varepsilon} \tag{24}$$

where τ_0 is the nominal delay, $\Delta\tau(t)$ is the variation around τ_0, and $\bar{\varepsilon}$ is the upper bound.

Proposition 2. Let $a \in \mathbb{R}$ and $b \in \mathbb{R}$ be two real scalars, where $a \neq 0$ and $a + b \neq 0$, then

$$(a+b)^{-1} = a^{-1} - a^{-1}\frac{b}{a+b} \tag{25}$$

Proof. Using some basic arithmetic operations, it can be shown, that (25) holds. □

Using Proposition 2, we can write

$$\frac{1}{\tau(t)} = \big(\tau_0 + \Delta\tau(t)\big)^{-1} = \frac{1}{\tau_0} - \frac{1}{\tau_0}\Delta\tau^*(t) \tag{26}$$

where $\Delta\tau^*(t) = \frac{\Delta\tau(t)}{\tau_0 + \Delta\tau(t)}$.

Problem 2 is solved using (26), that is

$$\hat{\boldsymbol{A}}_0 = \begin{bmatrix} \boldsymbol{A} & \boldsymbol{B}\boldsymbol{C}_d^{\tau_0} \\ \boldsymbol{0} & \boldsymbol{A}_d^{\tau_0} \end{bmatrix}, \ \Delta\hat{\boldsymbol{A}}(t) = \begin{bmatrix} \boldsymbol{0} & -\boldsymbol{B}\boldsymbol{C}_d^{\tau_0} \\ \boldsymbol{0} & -\boldsymbol{A}_d^{\tau_0} \end{bmatrix}\Delta\tau^*(t) \tag{27}$$

where $\boldsymbol{A}_d^{\tau_0} = -\frac{2}{\tau_0}\boldsymbol{I}$ and $\boldsymbol{C}_d^{\tau_0} = \frac{4}{\tau_0}\boldsymbol{I}$.

Similarly, as in previous section, the time-varying uncertainty is expressed as an unknown input $\boldsymbol{d}^2(t)$, which enters the augmented dynamics (22) through $\hat{\boldsymbol{E}}_{d_2}$, that is

$$\hat{\boldsymbol{E}}_{d_2}\boldsymbol{d}^2(t) = \Delta\hat{\boldsymbol{A}}(t)\boldsymbol{z}(t) = \underbrace{\begin{bmatrix} \boldsymbol{0} & -\boldsymbol{B}\boldsymbol{C}_d^{\tau_0} \\ \boldsymbol{0} & -\boldsymbol{A}_d^{\tau_0} \end{bmatrix}}_{\hat{\boldsymbol{E}}_{d_2}} \underbrace{\Delta\tau^*(t)\boldsymbol{z}(t)}_{\boldsymbol{d}^2(t)} \tag{28}$$

Now, the two unknown inputs $\boldsymbol{d}^1(t)$ and $\boldsymbol{d}^2(t)$ can be lumped together as in (14). Similarly for $\hat{\boldsymbol{E}}_{d_1}$ and $\hat{\boldsymbol{E}}_{d_2}$ as in (15). Furthermore, the system described by (22) can be rewritten as

$$\begin{aligned} \dot{\boldsymbol{z}}(t) &= \hat{\boldsymbol{A}}_0\boldsymbol{z}(t) + \hat{\boldsymbol{B}}\boldsymbol{u}^c(t) + \hat{\boldsymbol{E}}_f\boldsymbol{f}(t) + \hat{\boldsymbol{E}}_d\boldsymbol{d}(t) \\ \boldsymbol{y}(t) &= \hat{\boldsymbol{C}}\boldsymbol{z}(t) \end{aligned} \tag{29}$$

Note that (29) has the same structure as (16). The only difference is in the way how the time-varying uncertainty is handled in terms of UIs.

5. ROBUST RESIDUAL GENERATOR DESIGN BY USING EIGENSTRUCTURE ASSIGNMENT

In this section we focus on UI decoupling for discrete-time systems (16), however the same procedure can be used for decoupling of the UIs in continuous-time systems (29), with only difference that the observer eigenvalues will belong to a different set of stable eigenvalues.

In order to solve Problem 1, we define the following residual generator based on full-order observer

$$\begin{aligned} \hat{\boldsymbol{z}}_{k+1} &= (\hat{\boldsymbol{A}}_0 - \boldsymbol{L}\hat{\boldsymbol{C}})\hat{\boldsymbol{z}}_k + \hat{\boldsymbol{B}}_0\boldsymbol{u}_k^c + \boldsymbol{L}\boldsymbol{y}_k \\ \boldsymbol{r}_k &= \boldsymbol{Q}(\boldsymbol{y}_k - \hat{\boldsymbol{C}}\hat{\boldsymbol{z}}_k) \end{aligned} \tag{30}$$

where $\boldsymbol{r}_k \in \mathbb{R}^{n_p}$ is the residual vector and $\hat{\boldsymbol{z}}_k$ is the state estimation. The matrix $\boldsymbol{Q} \in \mathbb{R}^{n_p \times n_y}$ is the residual weighting matrix.

Defining the state estimation error $\boldsymbol{e}_k = \boldsymbol{z}_k - \hat{\boldsymbol{z}}_k$, the residual generator is governed by

$$\begin{aligned} \boldsymbol{e}_{k+1} &= (\hat{\boldsymbol{A}}_0 - \boldsymbol{L}\hat{\boldsymbol{C}})\boldsymbol{e}_k + \hat{\boldsymbol{E}}_f\boldsymbol{f}_k + \hat{\boldsymbol{E}}_d\boldsymbol{d}_k \\ \boldsymbol{r}_k &= \boldsymbol{H}\boldsymbol{e}_k \end{aligned} \tag{31}$$

where $\boldsymbol{H} = \boldsymbol{Q}\hat{\boldsymbol{C}}$. The Z-transformed residual response to faults and UIs is thus

$$\boldsymbol{r}(z) = \boldsymbol{G}_{rf}(z)\boldsymbol{f}(z) + \boldsymbol{G}_{rd}(z)\boldsymbol{d}(z) \tag{32}$$

where

$$\boldsymbol{G}_{rf}(z) = \boldsymbol{H}(z\boldsymbol{I} - \hat{\boldsymbol{A}}_0 + \boldsymbol{L}\hat{\boldsymbol{C}})^{-1}\hat{\boldsymbol{E}}_f \tag{33}$$

$$\boldsymbol{G}_{rd}(z) = \boldsymbol{H}(z\boldsymbol{I} - \hat{\boldsymbol{A}}_0 + \boldsymbol{L}\hat{\boldsymbol{C}})^{-1}\hat{\boldsymbol{E}}_d \tag{34}$$

Once $\hat{\boldsymbol{E}}_d$ is known, the remaining problem is to find the matrices $\boldsymbol{L}$ and $\boldsymbol{Q}$ to satisfy $\boldsymbol{G}_{rd}(z) = \boldsymbol{0}$. The assignment of the observer's eigenvectors and eigenvalues is a direct way to solve this design problem.

5.1 Unknown input decoupling by assigning left eigenvectors

Lemma 1. The transfer function $\boldsymbol{G}_{rd}(z)$ can be expanded in terms of the eigenstructure as

$$\boldsymbol{G}_{rd}(z) = \boldsymbol{H}(z\boldsymbol{I} - \hat{\boldsymbol{A}}_c)^{-1}\hat{\boldsymbol{E}}_d = \sum_{i=1}^{n} \frac{\boldsymbol{\Upsilon}_i}{z - \lambda_i} \qquad (35)$$

where $\boldsymbol{\Upsilon}_i = \boldsymbol{H}\boldsymbol{v}_i\boldsymbol{l}_i^T\hat{\boldsymbol{E}}_d$, $\boldsymbol{v}_i$ and $\boldsymbol{l}_i^T$ are the right and left eigenvectors of $\hat{\boldsymbol{A}}_c = \hat{\boldsymbol{A}}_0 - \boldsymbol{L}\hat{\boldsymbol{C}}$ associated with eigenvalue λ_i.

It is well known that, a given left eigenvector $\boldsymbol{l}_i^T$ of $\hat{\boldsymbol{A}}_c$ is always orthogonal to the right eigenvectors $\boldsymbol{v}_j$ corresponding to the remaining $(n-1)$ eigenvalues λ_j of $\hat{\boldsymbol{A}}_c$, where $\lambda_i \neq \lambda_j$.

Theorem 2. (Chen and Patton [1999]). If $\boldsymbol{Q}\hat{\boldsymbol{C}}\hat{\boldsymbol{E}}_d = 0$ and all rows of the matrix $\boldsymbol{H} = \boldsymbol{Q}\hat{\boldsymbol{C}}$ are left eigenvectors of $\hat{\boldsymbol{A}}_c$ corresponding to n_p eigenvalues of $\hat{\boldsymbol{A}}_c$, then $\boldsymbol{G}_{rd}(z) = \boldsymbol{0}$ is satisfied.

Proof. If the rows of $\boldsymbol{H}$ are n_p left eigenvectors $(\boldsymbol{l}_i, i = 1, \ldots, n_p)$ of $\hat{\boldsymbol{A}}_c$, i.e.

$$\boldsymbol{H} = \begin{bmatrix} \boldsymbol{l}_1 & \boldsymbol{l}_2 & \ldots & \boldsymbol{l}_{n_p} \end{bmatrix}^T \qquad (36)$$

then $\boldsymbol{H}\boldsymbol{v}_i = \boldsymbol{0}$ and $\boldsymbol{\Upsilon}_i = 0$ for $i = n_p + 1, \ldots, n$. If further we have $\boldsymbol{Q}\hat{\boldsymbol{C}}\hat{\boldsymbol{E}}_d = \boldsymbol{H}\hat{\boldsymbol{E}}_d = \boldsymbol{0}$, i.e. $\boldsymbol{l}_i^T\hat{\boldsymbol{E}}_d = \boldsymbol{0}$ and $\boldsymbol{\Upsilon}_i = 0$ for $i = 1, 2, \ldots, n_p$. Thus $\boldsymbol{G}_{rd}(z) = \boldsymbol{0}$. □

The first step for the design of an UI decoupled residual generator (30) is to compute the weighting matrix $\boldsymbol{Q}$ which must satisfy the following necessary condition (Chen and Patton [1999])

$$\boldsymbol{Q}\hat{\boldsymbol{C}}\hat{\boldsymbol{E}}_d = \boldsymbol{H}\hat{\boldsymbol{E}}_d = \boldsymbol{0} \qquad (37)$$

The necessary and sufficient condition for solution (37) to exist is $\text{rank}(\hat{\boldsymbol{C}}\hat{\boldsymbol{E}}_d) < n_y$. If $\hat{\boldsymbol{C}}\hat{\boldsymbol{E}}_d = \boldsymbol{0}$, any weighting matrix can satisfy this necessary condition. A general solution is

$$\boldsymbol{Q} = \boldsymbol{Q}_1(\boldsymbol{I} - \hat{\boldsymbol{C}}\hat{\boldsymbol{E}}_d(\hat{\boldsymbol{C}}\hat{\boldsymbol{E}}_d)^+) \qquad (38)$$

where $\boldsymbol{Q}_1 \in \mathbb{R}^{n_p \times n_y}$ is an arbitrary matrix and $(\hat{\boldsymbol{C}}\hat{\boldsymbol{E}}_d)^+$ is the pseudo-inverse of $(\hat{\boldsymbol{C}}\hat{\boldsymbol{E}}_d)$.

The second step is to determine the eigenstructure of the observer. The rows of $\boldsymbol{H}$ must be the n_p left eigenvectors of $\hat{\boldsymbol{A}}_c$. The remaining $n - n_p$ left eigenvectors can be chosen without restraint. For the given (stable) eigenvalue spectrum $\Lambda(\hat{\boldsymbol{A}}_c) = \{\lambda_i, i = 1, \ldots, n\}$, the following relation holds

$$\boldsymbol{l}_i^T(\lambda_i\boldsymbol{I} - \hat{\boldsymbol{A}}) = -\boldsymbol{l}_i^T\boldsymbol{L}\hat{\boldsymbol{C}} = -\boldsymbol{w}_i^T\hat{\boldsymbol{C}}, \quad i = 1, \ldots, n \qquad (39)$$

where

$$\boldsymbol{w}_i^T = \boldsymbol{l}_i^T\boldsymbol{L} \qquad (40)$$

The assignability condition says, that for each λ_i, the corresponding left eigenvector $\boldsymbol{l}_i^T$ should lie in the column subspace spanned by $\{\hat{\boldsymbol{C}}(\lambda_i\boldsymbol{I} - \hat{\boldsymbol{A}})^{-1}\}$, i.e. a vector $\boldsymbol{w}_i$ exists such that

$$\boldsymbol{l}_i^T = \boldsymbol{w}_i^T\boldsymbol{K}_i, \qquad i = 1, \ldots, n_p \qquad (41)$$

where

$$\boldsymbol{K}_i = -\hat{\boldsymbol{C}}(\lambda_i\boldsymbol{I} - \hat{\boldsymbol{A}}_0)^{-1}, \qquad i = 1, \ldots, n_p \qquad (42)$$

The projection of $\boldsymbol{l}_i$ in the subspace $\text{span}\{\boldsymbol{K}_i\}$ is denoted by:

$$\boldsymbol{l}_i^{\circ T} = \boldsymbol{w}_i^{\circ T}\boldsymbol{K}_i, \qquad i = 1, \ldots, n_p \qquad (43)$$

where

$$\boldsymbol{w}_i^{\circ T} = \boldsymbol{l}_i^T\boldsymbol{K}_i^T(\boldsymbol{K}_i\boldsymbol{K}_i^T)^{-1}, \qquad i = 1, \ldots, n_p \qquad (44)$$

If $\boldsymbol{l}_i^T = \boldsymbol{l}_i^{\circ T}$, $\boldsymbol{l}_i^T$ is in $\text{span}\{\boldsymbol{K}_i\}$ and is assignable. Otherwise, an approximative procedure must be taken, i.e. to replace $\boldsymbol{l}_i^T$ by it's projection $\boldsymbol{l}_i^{\circ T}$.

The remaining $n - n_p$ eigenvalues and corresponding eigenvectors can be chosen freely from the assignable subspace and assigned using some eigenstructure assignment technique, e.g. SVD decomposition. Then, the observer gain matrix $\boldsymbol{L}$ can be computed as follows:

$$\boldsymbol{L} = \boldsymbol{P}^{-1}\boldsymbol{W} \qquad (45)$$

where

$$\boldsymbol{W} = \begin{bmatrix} \boldsymbol{w}_1^\circ & \ldots & \boldsymbol{w}_{n_p}^\circ & \boldsymbol{w}_{n_p+1} & \ldots & \boldsymbol{w}_n \end{bmatrix}^T$$
$$\boldsymbol{P} = \begin{bmatrix} \boldsymbol{l}_1^\circ & \ldots & \boldsymbol{l}_{n_p}^\circ & \boldsymbol{l}_{n_p+1} & \ldots & \boldsymbol{l}_n \end{bmatrix}^T$$

It is obvious, that the first n_p eigenvalues corresponding to the required eigenvectors $\boldsymbol{l}_i^T, i = 1, \ldots, n_p$ must be real because all these eigenvectors are real-valued.

Remark 5. The remaining design freedom, after UI decoupling has been satisfied, can be used to optimize other performance indices such as fault sensitivity.

6. APPLICATION TO THE MSR MISSION

The applicative support of this paper concerns the Mars Sample Return (MSR) mission. It is a future exploration mission undertaken jointly by the National Aeronautics and Space Administration (NASA) and the European Space Agency (ESA). The goal is to take sample of the surface, the rocks and the atmosphere of Mars and to return these samples safe and intact back to Earth for analysis. Five spacecrafts are involved in this space mission: an Earth/Mars transfer vehicle, an ascent/descent module, a chaser spacecraft and an Earth re-entry vehicle.

Once the samples are collected, they are loaded on the Mars Ascent Vehicle (MAV) which is then launched into the Martian orbit around the planet to rendezvous with the chaser spacecraft. To a success of the rendezvous mission, the chaser vehicle uses Inertial Measurement Units (IMUs), a Star TRacker (STR), a LIght Detection And Ranging (LIDAR) sensor, a Radio Frequency Sensor (RFS), a Coarse Sun Sensor (CSS), and a very precise propulsion system composed of THRusters (THRs) and reaction wheels (RWs). The rendezvous mission can be in danger if a fault occurs in these thrusters, since the chaser may not compensate, for example, J2 disturbances and/or may lose the attitude and/or the position of the sample container containing the Mars's samples.

Such faulty situations cannot obviously be diagnosed by ground operators using telemetry information due to the potential lack of communication between the chaser and the ground stations or due to significant delays. This has motivated the development of onboard fault diagnosis solutions. As a result, two robust fault detection schemes presented in previous sections are now considered for the detection and isolation of faults occurring in the chaser's thrusters unit.

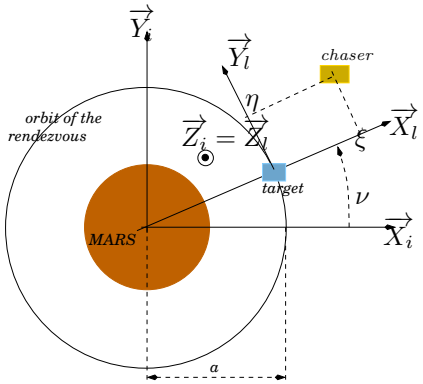

Fig. 1. The rendezvous orbit and associated frames

6.1 Modeling the chaser dynamics during the rendezvous

From the exhaustive space literature we only consider the necessary backgrounds on modeling the relative position of two spacecrafts on a circular orbit around a planet. The interested reader can refer to e.g. Wie [1998], Wertz and Larson [1999], Wisniewski [1999] for more details.

The motion of the chaser is derived from the 2nd Newton law. To proceed, let $a, m, \mathcal{G}$ and m_M denote the orbit of the target, the mass of the chaser, the gravitational constant and the mass of the planet Mars. Then, the orbit of the rendezvous being circular, the velocity of any object (e.g. the chaser and the target) is given by the relation $\sqrt{\frac{\mu}{a}}$, where $\mu = \mathcal{G}.m_M$.

Let $\mathcal{R}_l : (O_{tgt}, \overrightarrow{X_l}, \overrightarrow{Y_l}, \overrightarrow{Z_l})$ be the frame attached to the target and oriented as shown in Figure 1. Because the linear velocity of the target is given by the relation $a\dot{\theta}$ in the inertial frame $\mathcal{R}_i : (O_M, \overrightarrow{X_i}, \overrightarrow{Y_i}, \overrightarrow{Y_i})$ (those that is attached to the center of Mars), it follows:

$$a.\dot{\theta} = \sqrt{\frac{\mu}{a}} \Rightarrow n = \sqrt{\frac{\mu}{a^3}} \tag{46}$$

During the rendezvous phase, it is assumed that the chaser motion is due to the four following forces:

- the Mars attraction force $\overrightarrow{F_a}$ given in $\mathcal{R}_l$ by:

$$\overrightarrow{F_a} = -m\frac{\mu}{((a+\xi)^2+\eta^2+\zeta^2)^{3/2}}\Big((a+\xi)\overrightarrow{X_l}+\eta\overrightarrow{Y_l}+\zeta\overrightarrow{Z_l}\Big);$$

- the centripetal force $\overrightarrow{F_e} = m\Big(n^2\xi\overrightarrow{X_l} + n^2\eta\overrightarrow{Y_l} + 0\overrightarrow{Z_l}\Big);$
- the Coriolis force $\overrightarrow{F_c}$ in $\mathcal{R}_l$ is given by:

$$\overrightarrow{F_c} = m\left(2n\dot{\eta}\overrightarrow{X_l} - 2n\dot{\xi}\overrightarrow{Y_l} + 0\overrightarrow{Z_l}\right);$$

- and the forces due to the thrusters:

$$\overrightarrow{F_{thr}} = F_\xi\overrightarrow{X_l} + F_\eta\overrightarrow{Y_l} + F_\zeta\overrightarrow{Z_l}.$$

Then, from the 2nd Newton law, it follows

$$\begin{aligned}
\ddot{\xi} &= n^2\xi + 2n\dot{\eta} - \frac{\mu}{((a+\xi)^2+\eta^2+\zeta^2)^{3/2}}(a+\xi) + \frac{F_\xi}{m}\\
\ddot{\eta} &= n^2\eta - 2n\dot{\xi} - \frac{\mu}{((a+\xi)^2+\eta^2+\zeta^2)^{3/2}}\eta + \frac{F_\eta}{m}\\
\ddot{\zeta} &= -\frac{\mu}{((a+\xi)^2+\eta^2+\zeta^2)^{3/2}}\zeta + \frac{F_\zeta}{m}
\end{aligned} \tag{47}$$

where ξ, η, ζ denote the three dimensional position of the chaser (assumed to be a punctual mass) in $\mathcal{R}_l$.

Because the distance between the target and the chaser is smaller than the orbit a, it is possible to derive the so called Hill-Clohessy-Wiltshire equations from equations (47) by means of a first order approximation. This boils down to a linear six order state space model whose input vector is $\boldsymbol{u}(t) = (F_\xi\ F_\eta\ F_\zeta)^T$ and state vector $\boldsymbol{x}(t) = (\xi\ \eta\ \zeta\ \dot{\xi}\ \dot{\eta}\ \dot{\zeta})^T$. Now, projecting the thrust forces due to the eight thrusters that equip the chaser into the frame $\mathcal{R}_l$, it follows from (47):

$$\begin{aligned}
\dot{\boldsymbol{x}}(t) &= \boldsymbol{A}\boldsymbol{x}(t) + \boldsymbol{B}R(\hat{Q}_{tgt}(t), \hat{Q}_{chs}(t))\boldsymbol{M}\boldsymbol{u}^{thr}(t) + \boldsymbol{E}_w\boldsymbol{w}(t)\\
\boldsymbol{y}(t) &= \boldsymbol{C}\boldsymbol{x}(t) + \boldsymbol{v}(t)
\end{aligned}$$

where $\hat{Q}_{tgt}(t) \in \mathbb{R}^4$ and $\hat{Q}_{chs}(t) \in \mathbb{R}^4$ denote the attitude's quaternion of the target and the chaser, respectively. These quaternions are estimates from the navigation module. $\boldsymbol{M} \in \mathbb{R}^{3\times 8}$ refers to the (static) allocation module, $\boldsymbol{u}^{thr}(t) \in \mathbb{R}^8$ refers to the thrusters input and $R(\hat{Q}_{tgt}(t), \hat{Q}_{chs}(t))$ is the quaternion dependent rotation matrix. $\boldsymbol{x}(t) \in \mathbb{R}^6$ is the state vector defined previously, $\boldsymbol{y}(t) \in \mathbb{R}^3$ refers to the three-dimensional (relative) position measured by a LIDAR unit and $\boldsymbol{w}(t) \in \mathbb{R}^3$ refers to the spatial disturbances. The considered disturbances in this study are solar radiations, gravity gradient and atmospheric drag. $\boldsymbol{v}(t) \in \mathbb{R}^3$ denotes the measurement noise assumed to be a white noise with very small variance due to the technology used for the design of the LIDAR. $\boldsymbol{A}, \boldsymbol{B}, \boldsymbol{C}$ and $\boldsymbol{E}_w$ are matrices of adequate dimension.

The considered thrusters faults can be modeled in a multiplicative form according to

$$\boldsymbol{u}_f^{thr}(t) = (\boldsymbol{I}_8 - \boldsymbol{\Psi}(t))\boldsymbol{u}^{thr}(t) \tag{48}$$

where

$$\boldsymbol{\Psi}(t) = diag\{\psi_i(t)\} : 0 \leq \psi_i(t) \leq 1,\ \ i = 1, \ldots, 8$$

models the thruster faults, e.g. a locked-in-placed fault can be modeled by $\Psi_i(t) = 1 - \frac{c}{\boldsymbol{u}^{thr_i}(t)}$ where c denotes a constant value (the particular values $c = \{0, 1\}$ allows to consider open/closed faults) whereas a fix value of $\Psi_i(t)$ models a loss of efficiency of the i^{th} thruster. $\boldsymbol{\Psi}(t) = 0\ \forall t$ means that no fault occurs in the thrusters.

Taking into account some unknown but bounded delays induced by the electronic devices and the uncertainties on the thruster rise times due to the thruster modulator unit that is modeled here as an unknown time-varying delay $\tau(t) = \tau_0 + \Delta\tau(t)$ with a (constant) nominal delay τ_0 and upper bounded variation part $|\Delta\tau(t)| \leq \bar{\varepsilon}$.

Furthermore, considering $R(\hat{Q}_{tgt}(t), \hat{Q}_{chs}(t))\boldsymbol{M}\boldsymbol{u}^{thr}(t)$ as the input vector $\boldsymbol{u}(t)$ and approximating the fault model $R(\hat{Q}_{tgt}(t), \hat{Q}_{chs}(t))\boldsymbol{M}\boldsymbol{\Psi}(t)\boldsymbol{u}^{thr}(t)$ in terms of additive faults $\boldsymbol{f}(t) \in \mathbb{R}^3$ acting on the state via a constant distribution matrix $\boldsymbol{E}_f$ (then $\boldsymbol{E}_f = \boldsymbol{B}$), it follows that the overall model of the chaser dynamics that takes into account both the attitude $(Q_{chs}(t))$ and the relative position $(\xi\ \eta\ \zeta)$ of the chaser can be written in the form (1), i.e.:

$$\begin{aligned}
\dot{\boldsymbol{x}}(t) &= \boldsymbol{A}\boldsymbol{x}(t) + \boldsymbol{B}\boldsymbol{u}(t) + \boldsymbol{E}_f\boldsymbol{f}(t) + \boldsymbol{E}_w\boldsymbol{w}(t)\\
\boldsymbol{y}(t) &= \boldsymbol{C}\boldsymbol{x}(t) + \boldsymbol{v}(t)
\end{aligned} \tag{49}$$

6.2 Design of the FDI schemes

The both FDI schemes use the above derived model (49) to construct the residual generator of the form (30). The uncertainty caused by the unknown time-varying delay τ_k is handled as an unknown input entering the augmented system's dynamics, (16) resp. (29), through the distribution matrix $\hat{\boldsymbol{E}}_{d_2}$. The sampling period of the navigation module is $T = 0.1s$ and the numerical values of the nominal time delays have been determined to be one sampling period, i.e. $0.1s$ for the input vector $\boldsymbol{u}$. Since the spatial disturbances $\boldsymbol{w}$ have the same directional properties as the faults, i.e. $\boldsymbol{E}_w = \boldsymbol{B}$, the residual signal $\boldsymbol{r}_k$ cannot be decoupled from $\boldsymbol{w}$, thus the disturbance decoupling is not considered here, i.e. $\hat{\boldsymbol{E}}_d = \hat{\boldsymbol{E}}_{d_2}$.

- The first FDI scheme is based on a polytopic transformation of the uncertainty caused by the influence of the unknown time-varying delay τ_k. First, the model (49) is transformed into the discrete representation (16), with $l = 1$ and $m = 1$. It practically means, that the unknown delay τ_k is assumed to be in the closed interval $[T, 2T)$. The obtained distribution matrix $\hat{\boldsymbol{E}}_d \in \mathbb{R}^{9\times 144}$ has $\text{rank}(\hat{\boldsymbol{E}}_d) = 6$ and a large number of columns. Thus, a full column rank factorization is performed using SVD decomposition. Finally, the obtained distribution matrix is used in the residual generator design using left eigenvector assignment (see section 5.1).
- The second FDI technique is formulated using a first order Padé approximation of the input time delay. The necessary theoretical developments were presented in section 4. The distribution matrix $\hat{\boldsymbol{E}}_d$ is computed as in (28), with $\tau_0 = 0.1s$. That basically means, that after UI decoupling is achieved, the resulted residual generator (30), using this technique, is robust against the time variations $\Delta\tau(t)$ (uncertainty) around the nominal delay τ_0. Finally, the residual generator (30) is converted to discrete-time using a Tustin approximation and implemented within the nonlinear simulator of the MSR mission.

Remark 6. In order to compare the proposed approaches, for the second design method (Padé), the assigned eigenvalues were chosen to be close to ≈ -0.5. Then, after the discretization of the continuous residual generator, the obtained closed-loop eigenvalues (discrete) were used for the eigenvalues assignment of the first (polytopic) method.

6.3 The fault isolation method

The proposed isolation strategy is based on the following normalized cross-correlation criterion between the j^{th} residual signal r_k^j and the associated controlled thrusters open rate $u_k^{thr_i}$

$$\sigma_k^j = \arg\min_i \Big| \frac{1}{N} \sum_{l=k}^{k+N} (r_l^j - \overline{r^j})(u_l^{thr_i} - \overline{u^{thr_i}}) \Big|,\ i = 1...8 \quad (50)$$

where $\overline{r^j}$ and $\overline{u^{thr_i}}, i = 1\dots 8, j \in \{1, 2, 3\}$ denote the mean values of the r^j and u^{thr_i}. For real-time reason, this criterion is computed on a N-length sliding-window. The resulting index σ_k^j refers to the identified faulty thruster using the j^{th} residual signal.

6.4 Simulation results

The two FDI schemes are then implemented within the MSR "high-fidelity" industrial simulator, provided by Thales Alenia Space. The simulations are carried out all during the last 20m of the rendezvous phase. The navigation unit is not considered to deliver "perfect" measurements. We also assume time delays induced by the thruster modulator unit and spatial disturbances (i.e. gravity gradient, atmospheric drag, and solar radiation pressure).

The simulated fault scenarios correspond to a single thruster opening at 100%, thruster closing itself (locked-closed) and monopropellant leakage. To make a final decision about the fault, a simple threshold based decision test is applied to $||r(k)||$ and implemented within the simulator. The isolation strategy is computed according to (50) using $j = 1$. The strategy works as follows: as soon as the fault is declared, the cross-correlation criterion (50) is computed.

Figure 2 and 3 illustrate the behaviour of the residual norm $\|\boldsymbol{r}_k\|$ and the isolation criteria σ_k, for some faulty situations. For each simulation, the fault occurs at $t = 1100s$ and lasts $50s$. As it can be seen from the figures, after a small transient behaviour, all considered faults are successfully detected and (quite well) isolated by both FDI units. To compare the performance of the proposed FDI schemes "isolation time" (time from fault occurrence to fault isolation) was considered (see Table 1). The results in the table are almost identical, but the Padé has an improved isolation performance towards locked-closed fault situation. Note, that the occurrence of incipient or small size thruster faults (e.g. small monopropellant leakage) may be covered by control actions, and the early detection/isolation of them is clearly more difficult.

Table 1. Isolation time in seconds

Fault type	Location	Padé appr.	Polytopic
Opening at 100%	8	1.1s	1.1s
Opening at 100%	3	1.2s	1.2s
Locked-closed	6	2.0s	2.7s
Leakage (20%)	4	1.9s	1.9s

7. CONCLUSIONS

In this paper, the problem of fault diagnosis of a linear continuous-time systems with subject to time-varying input delays is investigated. Two residual-based schemes were proposed that are robust against the presence of unknown time-varying delays induced by the electronic devices, which has not been addressed before to the best of our knowledge. The idea of both proposed methods is to transform the uncertainty caused by delays into unknown inputs and decouple them by means of EA technique. The first method utilizes a Cayley-Hamilton theorem based transformation when the influence of uncertain time-varying delay is transformed into polytopic uncertainty, which as shown later, greatly facilitates further manipulation. The second approach relies on a first-order Padé approximation around the nominal delay, where the variation part is expressed as an unknown input. Simulation results from the "high-fidelity" industrial simulator are presented in order to show the efficiency and capabilities of the proposed methods. Despite the presence

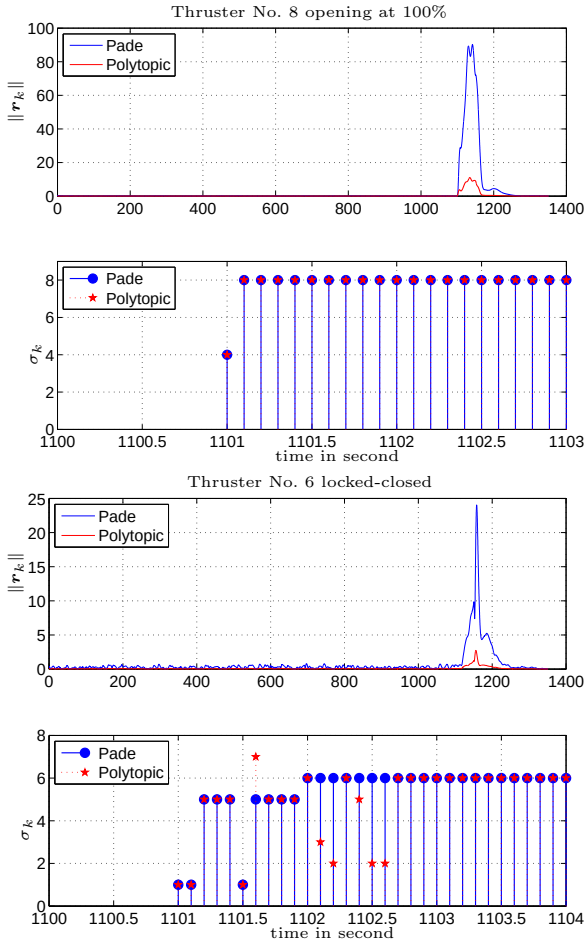

Fig. 2. Behaviour of the residual norm $\|\boldsymbol{r}_k\|$ and the isolation criteria σ_k for some faulty situations

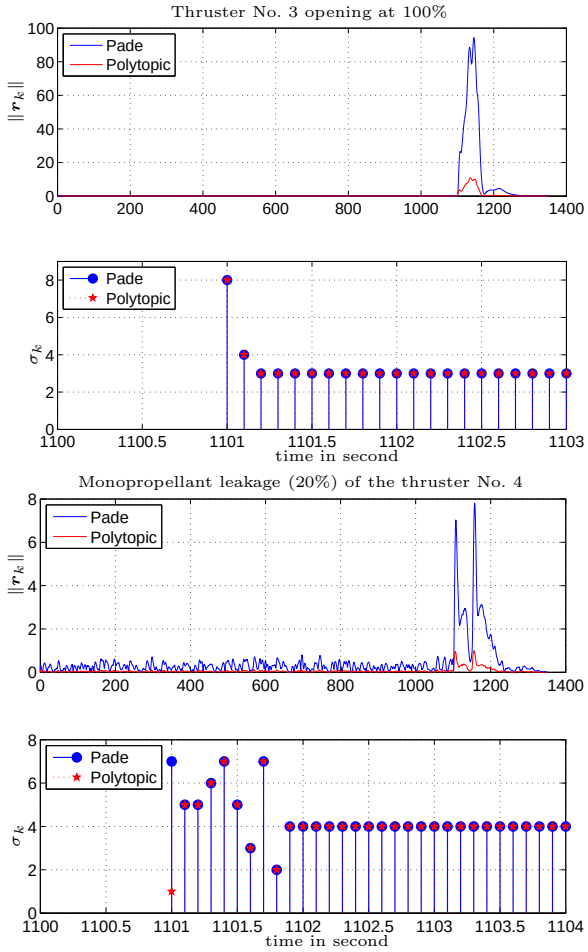

Fig. 3. Behaviour of the residual norm $\|\boldsymbol{r}_k\|$ and the isolation criteria σ_k for some faulty situations

of measurement noises, delays in the thruster modulator unit and spacial disturbances, the faults are successfully detected and isolated in a reasonable time.

ACKNOWLEDGEMENT

This research work was supported by the European Space Agency (ESA) and Thales Alenia Space in the frame of the ESA Networking/Partnering Initiative (NPI) Program.

REFERENCES

M. Blanke, M. Kinnaert, J. Lunze, and M. Staroswiecki. *Diagnosis and Fault-Tolerant Control*. Springer, 2006.

J. Chen and R. Patton. *Robust model-based fault diagnosis for dynamic systems*. Kluwer Academic Pub, 1999.

S.X. Ding. *Model-based fault diagnosis techniques: design schemes, algorithms, and tools*. Springer Verlag, 2008.

L. Hetel, J. Daafouz, and C. Iung. Stabilization of arbitrary switched linear systems with unknown time-varying delays. *IEEE Transactions on Automatic Control*, 51(10):1668–1674, 2006.

H.R. Karimi, M. Zapateiro, and N. Luo. A linear matrix inequality approach to robust fault detection filter design of linear systems with mixed time-varying delays and nonlinear perturbations. *Journal of the Franklin Institute*, 347(6):957–973, 2010.

I.E. Leonard. The matrix exponential. *SIAM review*, 38 (3):507–512, 1996.

N. Meskin and K. Khorasani. Robust fault detection and isolation of time-delay systems using a geometric approach. *Automatica*, 45(6):1567 – 1573, 2009.

Y.V. Mikheev, VA Sobolev, and E. Fridman. Asymptotic analysis of digital control systems. *Automation and Remote Control*, 49(9):1175–1180, 1988.

S. Olaru and S.I. Niculescu. Predictive control for linear systems with delayed input subject to constraints. In *IFAC World Congress*, Seoul, Korea, 2008.

J.D. Pintér. *Global optimization in action: continuous and Lipschitz optimization–algorithms, implementations, and applications*, volume 6. Springer, 1996.

Y. Wang, S.X. Ding, H. Ye, and G. Wang. A new fault detection scheme for networked control systems subject to uncertain time-varying delay. *IEEE Transactions on Signal Processing*, 56(10), 2008.

J.R. Wertz and W.J. Larson. *Space Mission Analysis and Design*. Space Technology Library. Springer, 1999.

B. Wie. Space vehicle dynamics and control(book). *Reston, VA: American Institute of Aeronautics and Astronautics, Inc, 1998.*, 1998.

R. Wisniewski. *Lecture Notes on Modeling of a Spacecraft*. Dep. of Control Engineering, Aalborg University, 1999.

H. Yang and M. Saif. Observer design and fault diagnosis for state-retarded dynamical systems. *Automatica*, 34 (2):217 – 227, 1998.